Geotechnical Engineering in the XXI Century: Lessons learned and future challenges
N.P. López-Acosta et al. (Eds.)

doi:10.3233/STAL190060

Characterization of Soil-Geosynthetic Interaction Properties Along Various Directions

M. M. ABOELWAFA[a,1], G. H. ROODI[a] and J. G. ZORNBERG[a]
[a] *Department of Civil, Architectural, and Environmental Engineering, The University of Texas at Austin*

Abstract. The recent introduction of geogrids with triangular apertures have raised questions regarding properties of these geogrids along various directions. This study presents the results of an experimental program conducted to determine soil-geosynthetic interaction properties in various directions of triangular and biaxial geogrids. Specifically, small-scale soil-geosynthetic interaction tests were conducted using a triangular geogrid and a biaxial geogrid and a uniform gravel backfill subjected to a normal pressure of 21 kPa. The geosynthetic specimens were cut in five directions including the machine and cross-machine directions, and at orientations of 30, 45, and 60 degrees between the machine and cross-machine directions. Ultimate pullout strength and the stiffness of the soil-geosynthetic composite (K_{SGC}) were obtained by using the soil-geosynthetic composite (SGC) model. Overall, it was found that the soil-geosynthetic interaction properties, including ultimate pullout resistance and K_{SGC}, were more uniform in the triangular aperture geogrid than the biaxial geogrid. Prediction by the SGC model also confirmed the above finding.

Keywords. Geosynthetics, base stabilization, soil-geosynthetic interaction, soil-geosynthetic composite model.

1. Introduction

Geosynthetics have been widely used in roadway systems, either by placing the geosynthetic at the interface of the base and subbase layers or at the interface of subbase and subgrade or within the unbound base course layer, to enhance the performance of paved roads under repeated traffic and environmental loads [1-4]. Use of geosynthetics in pavement structures has been aimed at fulfilling several functions including filtration, separation, lateral drainage, stiffening, and reinforcement [5, 6]. An important application of geosynthetics in roadway systems includes their use to stabilize the base and/or the subgrade. It is expected that inclusion of geosynthetic results in distribution of traffic load over a wider subgrade area, which consequently results in a comparatively lower maximum vertical stress on the subgrade. Contribution of geosynthetics to the performance of roadways has been expressed through three mechanisms: (1) lateral restraint of base course material, (2) increased bearing capacity, and (3) load transfer by the tensioned membrane effect [7-9]. The lateral restraint is considered the primary

[1] Corresponding author, Department of Civil, Architectural, and Environmental Engineering, University of Texas at Austin, 301 E. Dean Keeton, Austin, TX, USA; E-mail: m.aboelwafa@utexas.edu.

mechanism relevant to geosynthetic stabilization of base course. When a base course layer is subjected to repeated traffic loads, the granular particles of the base tend to spread laterally. The interaction between the geosynthetic layer and the base course particles, in form of interlocking and friction, provides additional confinement to the base course through lateral restraint mechanism.

A wide range of experimental and analytical approaches have been developed over the last three decades to enhance the knowledge on soil-geosynthetic interaction. Several test devices have been developed to evaluate soil-geosynthetic interface properties and understand the mechanisms involved in such interaction [10].

The soil-geosynthetic composite model (SGC) has recently been developed to provide an index parameter to characterize the stiffness of the soil-geosynthetic composite under small displacements [11,12]. The SGC model provides a closed-form analytical solution for geosynthetic displacements and its unit tension under confined conditions. This model relies on two parameters including the yield interface shear stress (τ_y) and the confined geosynthetic stiffness (J_c). This model assumes a linear relationship between the geosynthetic unit tension (T) and its tensile strain (ε) in the confined portion. The slope of the line has been referred to as the confined geosynthetic stiffness (J_c). The model also assumes a rigid-perfectly plastic interface shear with the yield interface shear stress referred to as τ_y. An important outcome of the SGC model was that it could capture both the tensile characteristics of the geosynthetic and the shear behavior of the soil-geosynthetic interface using a single parameter defined as the "*Stiffness of the Soil-Geosynthetic Composite* (K_{SGC})." A small-scale soil-geosynthetic interaction device has recently been adopted by the Univeristy of Texas at Austin to evaluate K_{SGC} for a wide range of geosynnthetics in the cross-machine and machine directions [13]. However, the effect of geosynthetic orientation on the soil-geosynthetic interaction properties has not extensively been studied. Gaining a better understanding on the soil-geosynthetic interaction properties along various directions is essential for geosynthetics that are subjected to multi-directional loads.

This study focuses on experimental evaluation of the impact of geosynthetic orientation on in-soil geosynthetic properties for triangular and biaxial geogrids. Specifically, small-scale soil-geosynthetic interaction tests were conducted along various directions of a triangular geogrid and a biaxial geogrid and the obtained results were used to provide a better understanding on the ultimate pullout resistance and the stiffness of the soil-geosynthetic composite, along different directions. The experimental observations were also compared to the predictions of the soil-geosynthetic composite model.

2. Materials and Experimental Setup

2.1. Geosynthetic Materials

A biaxial and triangular geogrid that were formed integrally from punched and drawn polypropylene sheets were used in this study (Figure 1). The triangular geogrid is referred to as GGT and the biaxial geogrid is referred to as GGB. Aboelwafa et al. has reported the manufacturer's specifications for the same triangular and biaxial geogrids tested in this study [14].

(a) 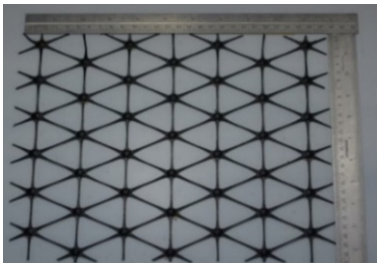 (b) 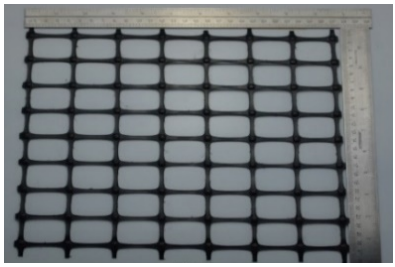

Figure 1. Geogrids used in this study: (a) triaxial or triangular (GGT); (b) biaxial (GGB).

2.2. Backfill Materials

The backfill material used in the soil-geosynthetic interaction tests was a uniform gravel referred to herein as AASHTO #8-Truncated. This material was sieved from a granular material that conformed to specifications of AASHTO Class 8 of aggregates as specified by AASHTO M43-05 [15]. The aggregate was composed of clean river-washed pea gravel with rounded particles that was obtained from Martin Marietta Sand and Gravel quarry in Garfield, Texas. Characteristics of AASHTO #8 and AASHTO #8-Truncated aggregates are summarized in Table 1.

Table 1. Properties of Backfill Materials used in this study.

Test	Index Parameter	AASHTO #8	AASHTO #8 (Truncated)
Soil Classification	-----	GP A-1-a	GP A-1-a
Specific Gravity	Specific Gravity, G_s	2.6	2.63
Grain Size Distribution	D_{10} (mm)	4.9	4.9
	D_{30} (mm)	6	5
	D_{50} (mm)	7	5.5
	D_{60} (mm)	7.5	5.65
	Cu	1.6	1.2
	Cc	1	0.9
Minimum Void Ratio	e_{min}	0.50	0.61
Maximum Void Ratio	e_{max}	0.70	0.80

2.3. Experimental Setup

The small-scale soil-geosynthetic interaction test machine used in this study had a number of the basic components of the traditional pullout equipment illustrated in the ASTM D 6706-01 [16]. However, the volume of soil utilized in the small-scale test was only 5 % of the soil volume required in the large pullout test with the minimum dimensions proposed in the ASTM standard. Moreover, the soil-geosynthetic interaction test equipment was designed to use in a vertical position because it was designed to be utilized with load frames suitable for wide-width tensile strength testing of geosynthetics. The soil-geosynthetic interaction tests were conducted at a constant displacement rate of 1 mm/min. Details of the testing procedure are described by Roodi et al. [13].

3. Experimental Results

The experimental results were used to estimate the ultimate pullout resistance and the stiffness of the soil-geosynthetic composite (K_{SGC}) for the two geogrids along the tested directions. The results along various directions are presented using a 360˚ radar chart. Specifically, the value presented at 0˚ angle corresponds to the soil-geosynthetic property obtained along the cross-machine direction (CD) and the value presented at 90˚ angle corresponds to the soil-geosynthetic property obtained along the machine direction (MD). The soil-geosynthetic properties obtained along 30˚, 45˚, and 60˚ directions (measured from CD in counterclockwise direction), are then presented at 30˚, 45˚, and 60˚ angles, respectively. For presentation purposes, the property values measured along 0˚, 30˚, 45˚, 60˚, and 90˚, were then duplicated around 360˚ (e.g., 30˚ matches 150˚, 210˚, and 330˚) to produce a 360˚ radar chart.

3.1. Pullout Load-Pullout Displacement Relationship

Soil-geosynthetic interaction tests were performed to evaluate in-plane soil-geosynthetic interaction properties. In this test, a pullout load was applied along the longitudinal direction of the engaged length under a confining pressure of 21 kPa (3 psi). The applied load and the resulting displacement of the specimen were measured. This load was then converted to the frontal unit tension, expressed in kN/m, by dividing by the engaged width of the geosynthetic specimen. Figures 2 and 3 show the frontal unit tension versus frontal displacement plots for the triangular and biaxial geogrids, respectively. Evaluation of the data presented in Figure 2 indicates a small difference among the curves obtained for various loading directions. This observation shows a generally similar soil-geosynthetic interaction response for the triangular geogrid along the directions tested.

On the other hand, Figure 3 shows that the frontal unit tension along directions other than MD and CD, was significantly smaller than along MD and CD for the biaxial geogrid. That may be attributed to the fact that the passive bearing resistance provided by the geogrid ribs in these directions were different from (and lower than) the passive bearing resistance provided by the transverse ribs in testing along machine and cross-machine directions.

3.2. Ultimate Pullout Resistance

In this section, the ultimate pullout resistance ratio along tested directions is discussed for each geosynthetic. This ratio was determined along different tested directions for each geosynthetic by dividing the ultimate pullout resistance along each tested direction by the ultimate pullout resistance in CD. Consistent with the ultimate unit tensions presented in Figure 2, Figure 4 shows that the ultimate pullout resistance ratio for the triangular geogrid is relatively uniform along all the tested directions. Specifically, the ultimate pullout resistance ratio for the triangular geogrid along various directions was found to range approximately from 0.975 to 1.035.

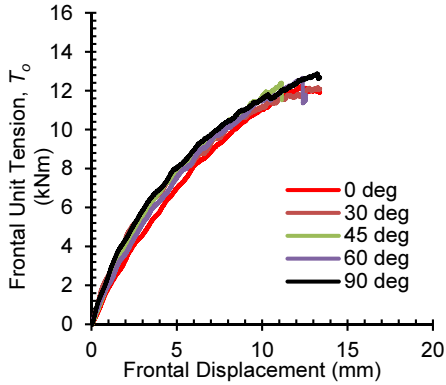

Figure 2. Frontal unit tension-displacement for the triangular geogrid.

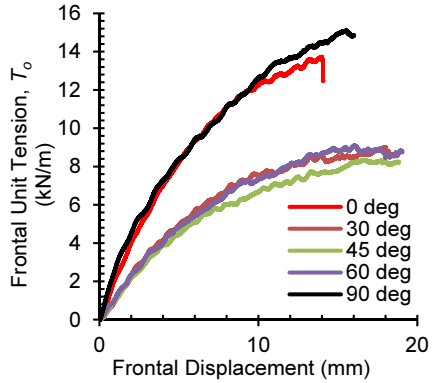

Figure 3. Frontal unit tension-displacement for the biaxial geogrid.

On the other hand, Figure 4 shows that the ultimate pullout resistance ratio for the biaxial geogrid highly depends on the direction of loading. When the pullout load was applied along the rib orientations (i.e., either the machine or cross-machine directions), the ultimate pullout resistance was noticeably high. Specifically, the ultimate pullout resistance along the machine direction was almost equal to the ultimate pullout resistance along the cross-machine direction, resulting an ultimate pullout resistance ratio of 0.974.

However, when the pullout load was applied along other directions (30˚, 45˚, and 60˚), the ultimate pullout resistance ratio was comparatively lower. The reason for the reduced ultimate pullout resistance ratio in 30˚, 45˚, and 60˚ directions can be attributed to the fact that the passive bearing resistance provided by the ribs in these directions were different from (and potentially lower than) the passive bearing resistance provided by the front of transverse ribs in machine and cross-machine directions. As shown in Figure 4, the ultimate pullout resistance ratio for the biaxial geogrid along various directions was found to range approximately from 0.636 to 1.

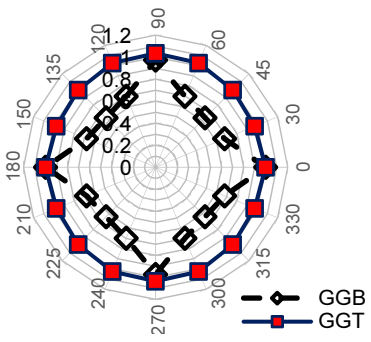

Figure 4. Ultimate pullout resistance ratio for geogrids.

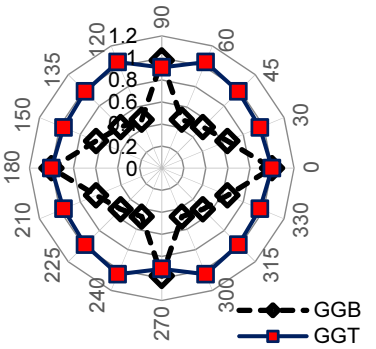

Figure 5. Stiffness of soil-geosynthetic composite ratio for geogrids.

3.3. Stiffness of Soil-geosynthetic Composite (K_{SGC})

In this section, the stiffness of the soil-geosynthetic composite ratio is discussed for each geosynthetic. A similar procedure to the one detailed for the ultimate pullout resistance was used to obtain K_{SGC} ratio. Figure 5 shows that the stiffness of the soil-geosynthetic composite ratio for the triangular geogrid is comparatively uniform along all tested directions.

Figure 5 also shows that the stiffness of the soil-geosynthetic composite ratio along various directions for the biaxial geogrid. Evaluation of the data presented in this figure indicates that the stiffness of the soil-geosynthetic composite for the biaxial geogrid in the machine direction was almost equal to that in the cross-machine direction. However, the stiffness of the soil-geosynthetic composite obtained along directions other than the machine and cross-machine directions, was significantly smaller. Although the reduced ultimate pullout resistance along these directions (presented in Figure 4) may partially explain the trend observed for the stiffness of the soil-geosynthetic composite, additional insights could be gained by investigation of the factors affecting the stiffness of the soil-geosynthetic composite. This investigation is presented next.

4. Comparison of Experimental Data with Predictions by SGC Model

This section compares observation from the soil-geosynthetic interaction test data for the stiffness of the soil-geosynthetic composite with the predictions based on the SGC model. According to the SGC model, the stiffness of the soil-geosynthetic composite is directly correlated with the product of confined geosynthetic stiffness (J) and the yield interface shear stress (τ_y) [11, 12]. A reasonable estimate for the yield interface shear can be obtained by dividing the ultimate pullout resistance by the contact area between soil and geosynthetic (or by dividing the ultimate frontal unit tension by two times the total length of the geosynthetic specimen). Figure 6 shows the variation of the yield interface shear stress ratio for the biaxial and triangular geogrids. This ratio was obtained by dividing the yield interface shear stress along each tested direction by that along the cross-machine direction.

On the other hand, estimation of the confined geosynthetic stiffness requires stress-strain measurements in the geosynthetic material along different testing directions. Using results obtained in a wide-width tensile test program, Aboelwafa et al. have reported tensile stress-strain data along various testing directions for the same triangular and biaxial geogrids tested in this study [14]. Figure 7 shows the ratio for tensile stiffness at 1% for the biaxial and triangular geogrids along various tested directions. This ratio was obtained by dividing the tensile stiffness along each tested direction by that along the cross-machine direction. Using the data presented in Figures 6 (for τ_y) and 7 (for J), predicted trend for K_{SGC} can be obtained using the product of τ_y and J for each geosynthetic. This data is presented in Figures 8 and 9 and is discussed next.

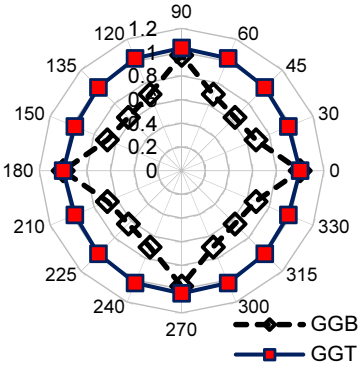

Figure 6. Yield interface shear stress ratio.

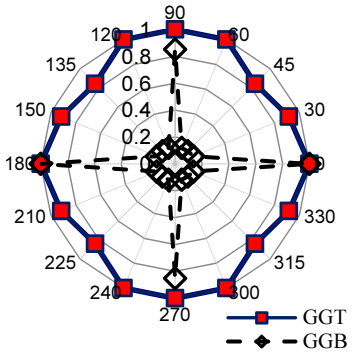

Figure 7. In-isolation tensile stiffness ratio.

4.1. Triangular Geogrid (GGT)

Figure 8 shows the stiffness of the soil-geosynthetic composite ratio obtained in the soil-geosynthetic interaction tests versus the same ratio predicted by the SGC model. Evaluation of the data presented in this figure indicates that the trend observed for K_{SGC} ratio in the soil-geosynthetic interaction test was very similar to that predicted from the SGC model. The consistency between observed and predicted trends was expected because uniform trends were observed for both τ_y and J. The K_{SGC} ratio obtained from the soil-geosynthetic interaction test data along tested directions ranged from 0.92 to 1.04, and the K_{SGC} ratio predicted by the SGC model ranged from 0.84 to 1.04.

4.2. Biaxial Geogrid (GGB)

Figure 9 shows the stiffness of the soil-geosynthetic composite ratio obtained in the soil-geosynthetic interaction tests versus the same ratio predicted by the SGC model. Although a reduced ratio along directions other than the machine and cross-machine directions were found in both data sets, these reduced ratios were not close to one another. The K_{SGC} ratio obtained from the soil-geosynthetic interaction test data along directions other than MD and CD ranged from 0.47 to 0.64, whereas the K_{SGC} ratio predicted by the SGC model for the same directions was approximately 0.1. A potential reason for the discrepancy between the measured and predicted K_{SGC} ratios for the biaxial geogrid along directions other than MD and CD could be the effect of confinement on the geogrid stiffness. The stiffness values obtained in the wide-width tensile tests (without soil confinement) are particularly low along directions other than MD and CD (Figure 7). This has been caused by the compression induced in a portion of biaxial geogrid ribs when they are loaded along directions other than their ribs. The induced compression eventually results in buckling and bending of these ribs. However, when the biaxial geogrid was loaded under confined condition, soil confinement would have partially mitigated (although not totally eliminated) buckling and bending of those ribs in compression. Consequently, for directions other than MD and CD, a comparatively larger J value, and thus a comparatively larger K_{SGC}, is expected for the soil-geosynthetic interaction test data (measured K_{SGC} values in Figure 9).

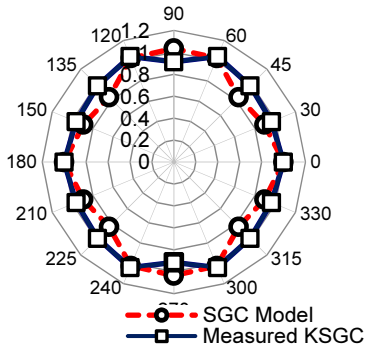

Figure 8. Measured vs. predicted K_{SGC} ratio (GGT).

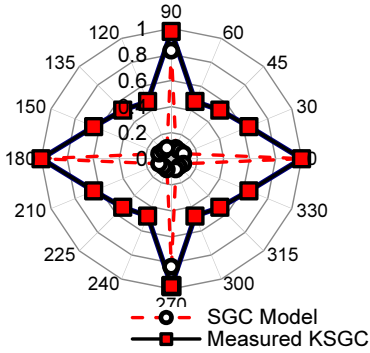

Figure 9. Measured vs. predicted K_{SGC} ratio (GGB).

However, when the biaxial geogrid was loaded along its ribs (i.e., CD or MD), the load was mainly transferred through the ribs oriented along the loading direction. Therefore, the effect of confinement on enhancement of geogrid stiffness was very small. Consistent with this expectation, the measured and predicted K_{SGC} ratios along the machine direction were very close (Figure 9). The K_{SGC} ratio obtained based on the SGC model was 0.83, whereas the K_{SGC} ratio obtained from the soil-geosynthetic interaction test (measured data in Figure 9) was slightly higher (0.98).

Overall, the trends obtained from both approaches underscore that the K_{SGC} ratio was particularly low along directions other than MD and CD.

5. Summary and Conclusions

The in-soil properties, including the ultimate pullout resistance and the stiffness of the soil-geosynthetic composite (K_{SGC}), of two types of geogrids, including a biaxial and a triaxial geogrid, were evaluated experimentally along five directions, including the machine and cross-machine directions and at orientations of 30, 45, and 60 degrees between the machine and cross-machine directions. All experiments were conducted using a small-scale soil-geosynthetic interaction test equipment.

The ultimate pullout resistance and the stiffness of the soil-geosynthetic composite (K_{SGC}) for the biaxial geogrid were found to be highly dependent on the direction of loading relative to the orientation of ribs. When the load was applied in the same direction as the orientation of the geogrid ribs, either machine or cross-machine directions, the ultimate pullout resistance and the stiffness of the soil-geosynthetic composite were high; but both parameters were significantly lower when the load was applied along other orientations.

The ultimate pullout resistance and the stiffness of the soil-geosynthetic composite (K_{SGC}) for the triangular geogrid were comparatively uniform along the multiple loading directions considered in this study.

Overall, comparison of the results obtained from the soil-geosynthetic interaction tests indicates that the triangular geogrid had comparatively more uniform soil-geosynthetic interaction properties along various directions than the biaxial geogrid. This finding suggests that triangular geogrids may be more suitable than biaxial geogrids for applications where loading in multiple (or random) directions are expected.

Acknowledgements

The first author is grateful for the financial support received from the U.S. Department of State (Fulbright Foreign Student Program). Support from Tensar is also greatly appreciated.

References

[1] Perkins, S.W. (2002). "Evaluation of Geosynthetic Reinforced Flexible Pavement Systems Using Two Pavement Test Facilities." *Montana DOT*, Report No. FHWA/MT-02-008/20040, Helena, Montana, USA.

[2] Al-Qadi, I.L., Dessouky, S.H., Kwon J. and Tutumluer, E. (2008), "Geogrids in Flexible Pavements: Validated Mechanisms", Transportation Research Record, No. 2045, Washington, D.C., 2008. pp. 102-109

[3] Zornberg, J. G. (2011). "Advances in the Use of Geosynthetic in Pavement Design." Invited Keynote Paper, Geosynthetics India '11, India Institute of Technology Madras, Chennai, India, Vol. 1, 3-21.

[4] Zornberg, J. G., Roodi, G. H., Ferreira, J. and Gupta, R. (2012a). "Monitoring Performance of Geosynthetic-Reinforced and Lime-Treated Low-Volume Roads under Traffic Loading and Environmental Conditions." *Geo-Congress 2012,* Oakland, CA, USA, 1310-1319.

[5] Koerner, R. M. (2012). *Designing with Geosynthetics*, 6th ed. Pearson Prentice Hall, 796p.

[6] Zornberg, J. G., Roodi, G. H., Sankaranarayanan, S., and Hernandez-Uribe, L. A. (2018). "Geosynthetics in roadways: Impact in sustainable development" Keynote Lecture, ICG 2018, Seoul, Korea, September 16-21.

[7] Holtz, R. D., Christopher, B. R. and Berg, R. R. (1998). "Geosynthetic design and construction guidelines." *U.S. Department of Transportation, Federal Highway Administration*, Washington, DC, FHWA-HI-98-038.

[8] Giroud, J. P., Ah-Line, C., and Bonaparte, R. (1984). "Design of unpaved roads and trafficked areas with geogrids." *Polymer Grid Reinforcement,* Thomas Telford, London, England, 116-127.

[9] Perkins, S. W. and Ismeik, M. (1997). "A Synthesis and Evaluation of Geosynthetic-reinforced Base Course Layers in Flexible Pavements: Part II Analytical Work." *Geosynthetics International*, 4(6), 605-621.

[10] Palmeira, E.M. and Milligan, W. E. (1989). "Scale and other factors affecting the results of pull-out tests of grids buried in sand." *Geotechnique*, 39, 511-524.

[11]Zornberg, J. G., Roodi, G. H., and Gupta, R. (2017). "Stiffness of Soil-Geosynthetic Composite under Small Displacements: I. Model Development." *Journal of Geotechnical and Geoenvironmental Engineering*, ASCE, Vol. 143, No. 10, 10.1061/(ASCE)GT.1943-5606.0001768, 04017075.

[12] Roodi, G. H., and Zornberg, J. G. (2017). "Stiffness of Soil-Geosynthetic Composite under Small Displacements: II. Experimental Evaluation" *Journal of Geotechnical and Geoenvironmental Engineering, ASCE*, Vol. 143, No. 10, 10.1061/(ASCE)GT.1943-5606.0001769, 04017076.

[13] Roodi, G. H., Zornberg, J. G., Aboelwafa, M. M., Phillips, J. R., Zheng, L., and Martinez, J. (2018). "Soil-geosynthetic Interaction Test to Develop Specifications for Geosynthetic-stabilized Roadways," *Center for Transportation Research (CTR),* Report No. FHWA/TX-17/5-4829-03-R1, Austin, Texas, 112 p.

[14] Aboelwafa, M.M., Roodi, G.H., and Zornberg, J.G. (2019). "In-Isolation Properties of Biaxial and Triangular Geogrids along Various Directions." *Geosynthetics 2019,* Houston, TX, USA.

[15] AASHTO M 43-05 (2013). "Standard Specification for Sizes of Aggregate for Road and Bridge Construction." A*merican Association of State Highway and Transportation Officials*, Washington, D.C., USA.

[16] ASTM D6706 (2007). "Standard Test Method for Measuring Geosynthetic Pullout Resistance in Soil." American Society for Testing and Materials, West Conshohocken, PA, USA, 8p.